Isogrid Structure Design and Mass-Strength Optimization in Airplane Lids

Mahmut ALKAN[1], Erhan CELIK[2], Ahmet Alp SUNECLI[3], Umut CAN[4], Sinan Barkin KOCADAG[5]

[1]Assoc. Prof., Nigde Omer Halisdemir University, Department of Mechanical Engineering, 51245 Nigde, Turkey
[2,3,4,5]Student, Nigde Omer Halisdemir University, Engineering Faculty, Department of Mechanical Engineering, 51245 Nigde, Turkey

---***---

Abstract - *Nowadays, along with the search for high performance materials and structures, the use of low mass and high mechanical resistant structures is of great importance. The aviation industry demands on components that are strong, light and can withstand very high loads. Within the scope of this study, a lid design study that can operate under high G force has been carried out for aircraft and spacecraft, taking into account the mass, hardness, strength and damage tolerance properties. In this study, optimization studies were carried out on aircraft lids with isogrid structures that have strengthening effect. The part produced for this purpose was used and tested for evaluation of production and design. As a result of this study, it was possible to produce a lighter aircraft lid without any loss of strength thanks to the isogrid structure. Analyzes have been verified as a result of the tests carried out on the prototypes of the final design*

Keywords: Isogrid, Isogrid Design, Aircraft Lids, Mass Optimization, Strength Optimization

1.INTRODUCTION

The low mass structure requirement of the aviation industry has led to a constant search. Grid structures are highly preferred structures especially in terms of mass savings. Isogrid structures, one of the types of grid structures, are advanced shell structures. Reinforcements arranged in equilateral triangles show high stability and rigidity, especially when these structures are made of composite material, with relatively low material input [1]. The complex mechanical behavior of isogrids must be known to optimize the hardener geometry. In this study, a small lid with a small number of hardeners was designed and studied. The study demonstrates conclusions about the behavior of the stiffeners intersections, the interaction between skin and reinforcement. As a result of the analyzes made, it has been determined that a critical malfunction is caused especially as a result of local buckling of the skin.

In the beginning, AA7050 was used as a building material as a result of the grinding process to obtain an isogrid structure. However, since Aluminum could not meet the lightness and cost characteristics, they were replaced by composite, which is a light and inexpensive material. Composite is a superior material in terms of high chemical and mechanical strength. In addition, their specific strength is higher than AA7050 [1]. However, due to the difficulties and problems encountered in the production of composite materials, a study was carried out with AA7050 material.

In this study, it is aimed to reduce the structural mass for the AA7050 material used in aircraft lids, thanks to isogrid structures and to improve their load carrying capabilities. Different grid structures were examined, and after the most suitable structure was determined, an isogrid structure reinforced aircraft landing gear lid was designed. At the end of the study, the prototype aircraft lid with isogrid structure was subjected to tests and verified with the analysis results. A lighter lid was designed and manufactured without strength reduction and without material changes.

2. INVESRIGATION of GRID STRUCTURES

Grid structures are types of partially carved structures with ribs of different geometries, usually consisting of a single metal plate or surface plate. These structures are shell-like structures that support the outer surface of any structure. Thanks to these structures, the mass of the designs can be reduced.

More strength can be obtained than other hollow designs. By using grid structures, the skin thickness and the load of the part can be reduced, this gives the damage-resistant and lighter design concept for aerospace structures. It also forms the basis of future adaptable structures. Aerospace grid structures contain load lids and reinforcements that must support the full mass of the upper stages and loads under high G loads. The strength of the part to be designed changes if it is formed with different geometries. Other grid types are formed by combining these grid structures, changing beam angles and removing beams on a certain axis. Of these structures, the isogrid structure has both vertical and horizontal beams and angled beams [2]. For this reason, they are resistant to forces acting both vertically and horizontally and at different angles. Isogrid structures are formed by the combination of orthogrid and anglegrid structures. Isogrid structures show their effect in the areas where these two grid structures are resistant. The ribs of the isogrid structure are unidirectional. Therefore, they do not delaminate and the crack is unlikely to spread in the space between the ribs or at the skin and interface between the ribs [2].

It is added to flat or curved sheet metal panels to increase out-of-plane bending stiffness. It is resistant to axial loads due to additional cross-sectional areas and redundant load paths. Aircraft lids must be resistant to pressure variation and airflow effects. In addition to this desired feature, it is desired that the lids can be opened and closed easily and that

the lids opening mechanisms consist of smaller systems. Supporting the outer layer of isogrid structures creates positive results for these requirements. The images of the basic grid geometries are given in **Figure 1.**
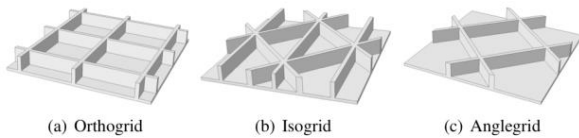

Figure -1: Basic grid structure geometries [1]

3. ISOGRID BUILDING DESIGN

The design was carried out in two stages. In the first stage, the iteration method was used to define the rib size of the lattice structure, while the material and thickness of the shell were determined by FEM (Finite Element Method) [1] in the second stage. In order to carry out the tests of the designed isogrid structure, the production process was planned and the details were determined.

Finally, the designed part is manufactured and tested to evaluate the quality of the manufacturing process and it is compliance with design requirements. While designing the isogrid structure, many different sizes of designs were made and comparisons were made with each other. The final isogrid aircraft lid is designed where the mass is the lowest and the strength is at the desired level. While evaluating the analysis results, attention was paid to ensure that the displacement was at most 1 mm.

The material used was 7050 series aluminum, which is one of the most preferred materials in the aviation industry. While determining the analysis boundary conditions, it was thought that one long side of the lid would be connected to the aircraft with a built-in hinge and the other long side would be opened and closed with a mechanism holding it in the middle.

The dimensions of the isogrid reinforced aircraft landing gear lid created in the final design were determined as 1500x150x7.5 mm. The plate thickness of this lid is 2.5 mm and the isogrid grilled part is 5 mm high. During the design, the isogrid structure was modeled starting from 20 mm inwards so that the landing gear lid could fit inside as per the design. The CAD view of the design is given in **Figure 2.**

Figure -2: Isogrid aircraft lid CAD design image
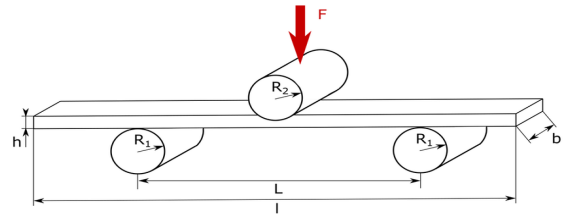
EXPERİMENTAL STUDIES

A. Three Point Bending Test

Figure -3: Three-point bending test setup diagram [3]

F: Force measured by load cell

R₁: Support roller diameter

R₂: Load cell cylinder diameter

L: Distance between supports

l: Tested sample size

h: Thickness of sample tested

b: Width of sample tested

Considering the ASTM E290-14 [4], ASTM E855-21 [5], ASTM D790-17 [6] standards in the three-point bending test, it is recommended that the ratio of L/h (the ratio of distance between supports to thickness of sample tested) be greater than 32.

At the same time, it is expected that the maximum test sample thickness h will be between 1-10 mm, the maximum loaded force value will be 30 kN, and the maximum mass will be 20 kg. The length of the test piece used in the tests is 346 mm, its width is 150 mm, the thickness of the lower sheet part is 2.5 mm, the height of the isogrid part is 5 mm and the total maximum thickness is 7.5 mm. The test sample used in the tests was designed by taking the length of 346 mm of the designed prototype part and produced from the same material as the prototype part. The rib thickness is 1.6 mm and 11 holes, 5 mm in diameter, are drilled for the built-in hinge. Production 346x150x7.5 mm profile was produced from AA7050 T7451 material with a thickness of 7.5 mm by milling. The test sample produced with AA7050 is shown in **Figure 4.**

Figure -4: Isogrid structure test sample

The thickness (h) value of the isogrid part used in the tests varies throughout the whole structure. For this reason, **Equation 1-1** taken from Meyer RR, Harwood OP, Harmon MB, Orlando JI (1973) Isogrid design handbook NASA book [2] was used for part thickness value determination.

$$\text{Equivalent Mass Thickness (mm)} = \bar{d} = \frac{\text{Volume (İsogrid)}}{\text{Area (Skin)}}$$
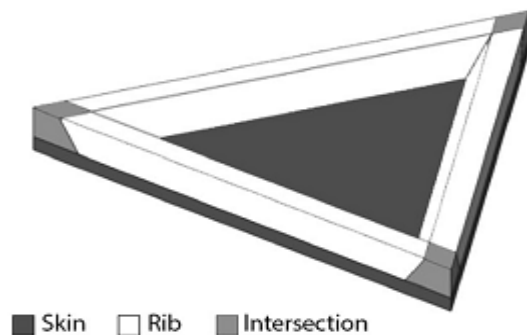
Equation 1-1

Figure -5: Single cell view of the isogrid structure [2]

The volume and skin area values of the isogrid structure used in the tests were determined for the AA7050 material from the CAD program of the part designed as 158674.58 mm^3 and 27636.62 mm^2, respectively. When the related equation was written instead of the values, our newly obtained thickness value (h) was determined as 158674.58/27636.62 and 5.742 mm. When our distance between supports (L) is taken as 220 mm, our L/h value is calculated as 220/5.742=38.31. Since the calculated value is greater than 32, the distance between the supports (L) was determined as 220 mm in the three-point test.

The test machine used in the three-point test was SHIMADZU AG-IS 100 kN with electric motor, the test setup was carried out with the load cell cylinder diameter and support cylinder diameters of 30 mm and the test speed was set as 5 mm/min. Three point bending test moment of the designed sample is shown in **Figure 6.**
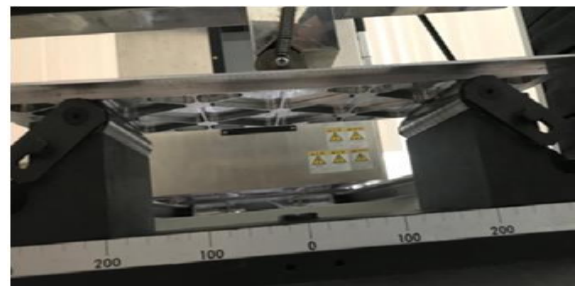

Figure -6: Three-point bending test movement

The three-point bending test was performed three times. The results obtained after the experiment are shown in **Table 1.** The data were obtained from the experimental device by means of the TRAPEZIUM2 program. Force F (N) - Stroke (mm) data for the three samples tested are given in **Graph 1.**

Table -1: Data obtained as a result of the three-point experiment

	Max. Force (N)	Max. Disp (mm)	Max. Stress (MPa)	Max. Strain (%)	Break Force (N)	Break Strain (%)
Specimen 1	2808,75	41,4160	109,853	3,85066	2806,25	3,86107
Specimen 2	2729,22	39,1418	106,743	3,63979	2723,91	3,64407
Specimen 3	2716,41	41,2050	106,242	3,83104	2711,56	3,83458
Average	2751,46	40,5876	107,6126	3,77383	2747,24	3,78
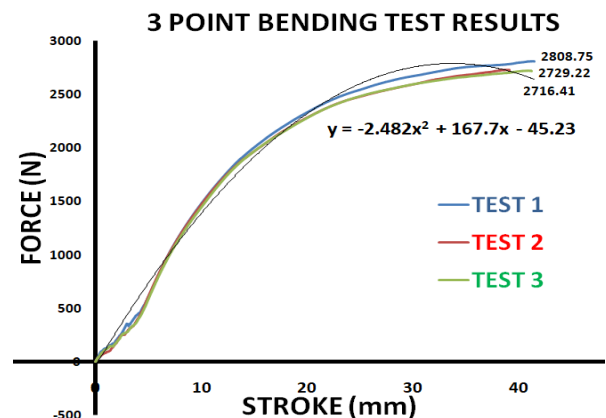
Graph -1: Three point bending test results

After the test, the ribs in the center of the isogrid structure showed a break in the back of the middle part where the force was applied in three samples. The specimens after the three-point bending test are shown in **Figure 7.** and the area where the crack occurred is shown in **Figure 8.** Experiment results were confirmed by computer analysis. The computer analysis result is shown in **Figure 9.**
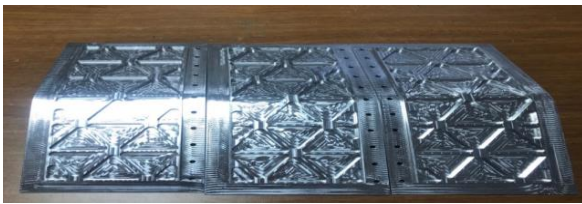
Figure -7: Post-experimental samples

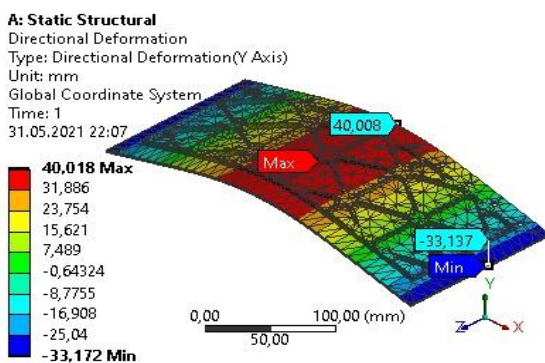

Figure -8: Crack images in the experiments

Figure -9: Three-point test computer analysis result

B. Springback Test Results

During the three-point bending test, it is an experiment in which the amount of stretching of the samples at maximum load and the amount of stretching after the force is removed are compared [7]. As a result of the experimental studies, the spring-back values of the aluminum sample, the bending angle values at the maximum load after the test device was manually brought back to the maximum load state, and the angle values after the load was removed were measured with the INSIZE degree-centered precision protractor 0-360 degrees 2372. The springback angles were obtained by subtracting the angle of twist from the measured angle. The schematic representation of the springback is listed in **Figure 10.** and the measurement results for three samples are listed in **Table 2**. An average springback angle of 13.333 degrees occurred.
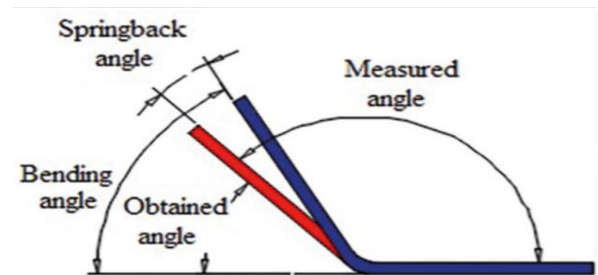

Figure -10: Springback schematic representation [7]

Table -2: Springback Results

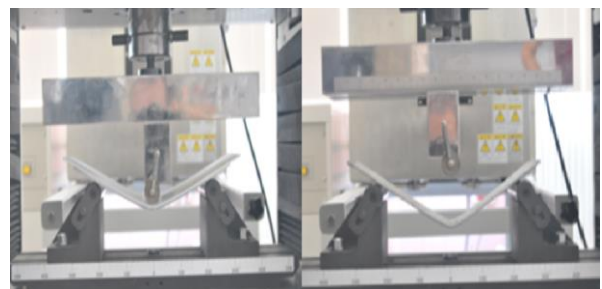|	Bending Angle	Obtained Angle	Springback Angle
1.	43	31	12
2.	45	30	15
3.	44	31	13
Average	44	30.66	13.33

Figure -11: Maximum force and condition after force removed

C. Buckling Experiment Results

It is observed that the machine elements shorten in length (according to Hooke's law until the elastic limit) with the compression forces acting along the axis direction [8]. If the force is increased further, it can be observed that the bar becomes unstable and cannot be restored due to insufficient rigidity, and it is subject to deformation (buckling) with the effect of the moment created by the force in the middle region of the bar. The deformation due to buckling occurs in different ways depending on the way the bars are supported. The critical load trying to buckling the bar depends on the material stiffness, the modulus of elasticity (E) and the bar geometric dimensions. The buckling test fastening types are shown in **Figure 12.**

Figure -12: Buckling test fastening types [9]

The test pieces used in the experiment are the same as the three point test. The experiment was repeated three times. Built-in buckling tests were carried out. The force loading rate was determined as 5 mm/min. The test machine used in the buckling test was SHIMADZU AG-IS 100 kN with electric motor. The data were obtained from the experimental device by means of the TRAPEZIUM2 program.
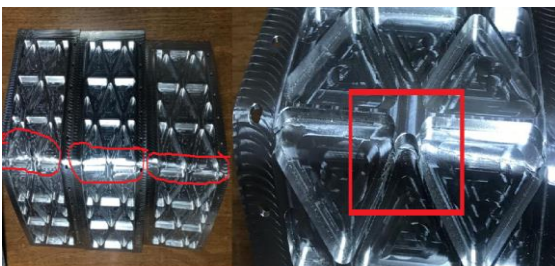


Figure -13: Regions where fracture is observed

The fractures occur in the ribs in the middle where the buckling starts, can be seen in **Figure 13.** As a result of this experiment, it was revealed that in case of a possible buckling, the first fractures will occur in the ribs and the rib thickness should be increased. The results obtained for the three samples are listed in **Graph 2, Graph 3** and **Graph 4.**
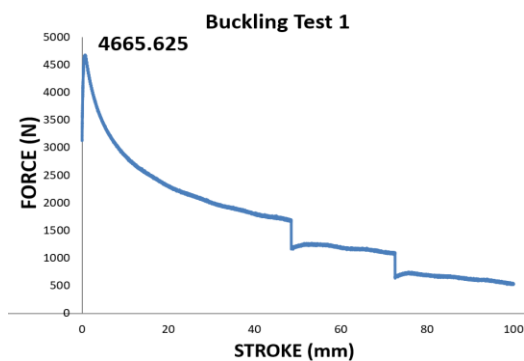
Graph -2: Force (N) – Stroke (mm) graph for the first sample
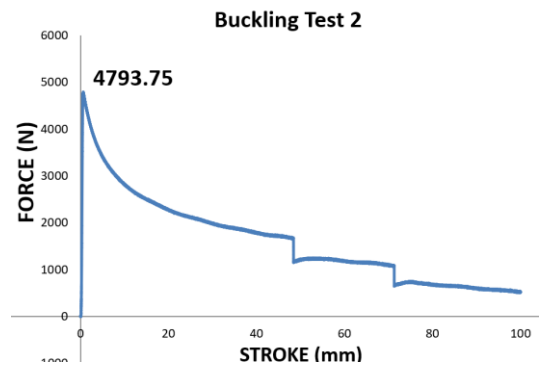
Graph -3: Force (N) – Stroke (mm) graph for the second sample
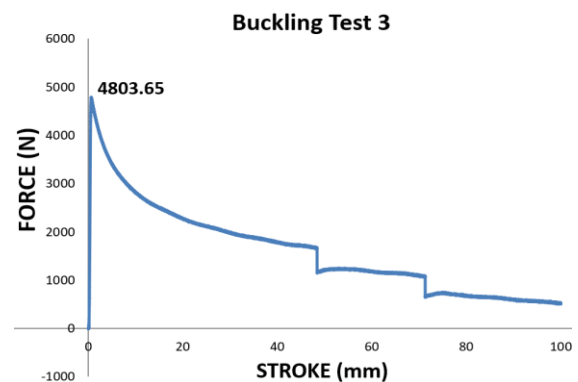
Graphic -4: Force (N) – Stroke (mm) graph for the third sample

As seen in **Graph 2, Graph 3** and **Graph 4**, sudden force drops between 45-50 mm and 70-75 mm occurred due to cracks in isogrid structures. While the graphs obtained as a result of the experiment continued homogeneously, they showed a sudden decrease. It has been concluded that the reason for this is the breaking of the isogrid structures that serve as the support, thus contributing to the delay of the fragment's breakage. The force data obtained as a result of the experiments and computer analyzes are shown in **Table 3**.

Table -3: Buckling forces obtained as a result of the buckling test

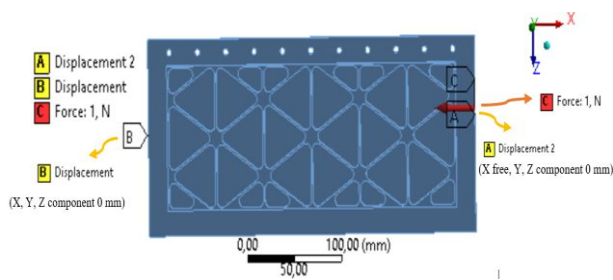|	**Buckling Force (N)**
Test 1	4665,625
Test 2	4793,75
Test 3	4803,65
Computer Analysis	4828,9

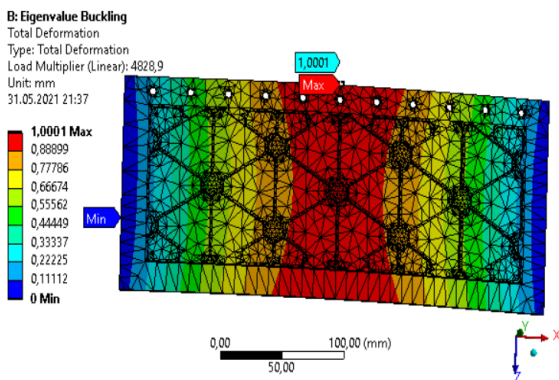**Figure -14:** Boundary conditions based on the buckling test analysis

Figure -15: Data obtained as a result of the analysis made in the computer environment (Load Multiplier value 4828.9 N)

The experiments performed and the analyzes made in the computer environment matched each other and the results of the experiments were confirmed. The computer analysis result is shown in **Figure 15.**

The load applied to the isogrid structural samples during the buckling test increased with displacement up to a peak reached at the onset of the buckling. Due to their geometric properties, isogrid structures have undergone local and global buckling.

D. Free Vibration Experiment Results

**Figure -16:** Free vibration test moment

Free vibration test has been carried out on the prototype plane lid, which is designed in the size of 1500x150x7.5 mm shown in **Figure 15.** In the test device, a test device with the

dimensions of the bottom table of 800x600x200 mm, the dimensions of the shaking table 500x500x10 mm and a working capacity of minimum 50 kg was used. In the experimental setup, the part with the isogrid structure was fixed from a   40x8 mm surface right in the middle of the long side without hinge holes. By creating an impact effect on the part from a 40x8 mm surface, the behavior of the vibration on the part over time was examined. As a result of the time-dependent variation of the vibration frequency and amplitude occurring in the system with the effect of the natural frequency, the vibration movements in the part were observed experimentally.

Table -4: Shaking table technical specifications

PROPERTY	Value	Unit
Piston Stroke	20	cm
Max. Displacement	±10	cm
Max. Acceleration	±2	g
Max. Piston Velocity	500	mm/s
Operating Frequency		
in ±80 mm operation	1	H
in ±2 mm operation	10	H
Servo Motor Power	750	W
Endless Screw Shaft	5	mm/dev
Screw Nut Dynamic Load Bearing Coefficient	60	kg.f

A servo motor with Schnieder Electric M0 1.4 Nm Nmax 8000 rpm PN 0.747 kW Imax 5.97 Arms features was used as Servo Motor, TESTBOX 2010 24-bit resolution, vibration sensitivity up to 2000 mV/g, internal noise of the system 5μg/√Hz, Multi-channel digitizer with sensor dimensions smaller than 111x65x60 mm, dynamic measuring range of at least 130 dB, +12V -12V voltage protection, compatible with MEMS,IEPE-ICP type and Strain Gauge based sensors, In the free vibration test, the FFT graph was created by performing the Fourier Transform. As a result, various types of frequency activity are shown in the piece with the help of graphics. The time graph, on the other hand, enables the observation of the change in position with the effect of the force exerted by the damper on the part over time.
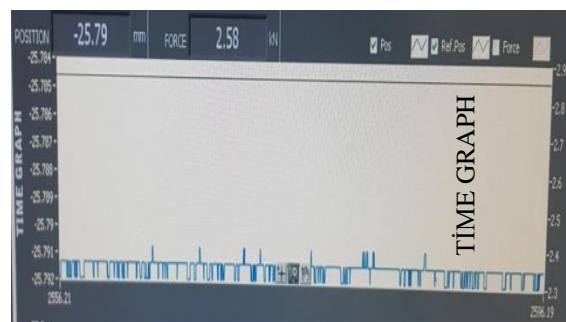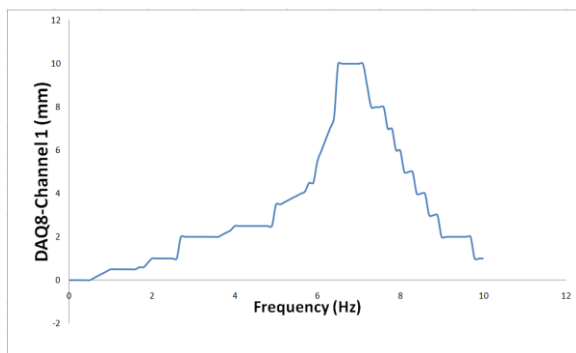

(a)
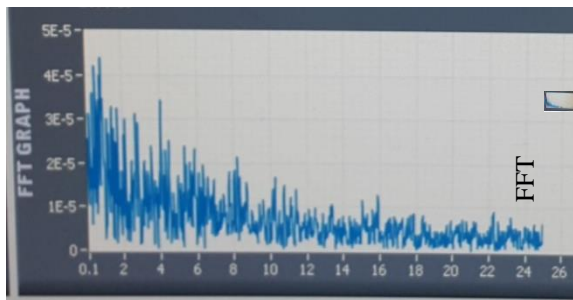
(b)

Graphics In experiments, (a) Time and (b) FFT graphs were obtained.

Table -5: Data defined in the TESTLAB shaking pad

STEP		SINE	
Step Size (mm)	50	Amplitude (mm)	0,5
Speed (mm/s)	20	Frequency (Hz)	6,8
		Cycles	500
POSITION (mm)	-25,79	FORCE (kN)	2,58

Graph -5: Frequency (Hz) and DAQ8- Channel1 (mm) graph obtained from free vibration test
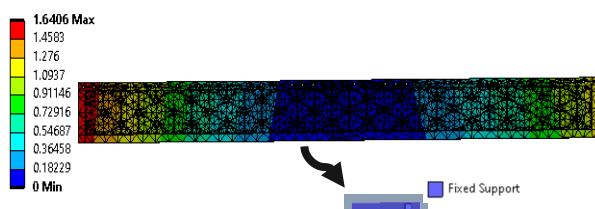

Figure -17: Vibration frequency data obtained as a result of computer analysis.

As a result of the data obtained from the free vibration experiment, it was observed that the first modal frequency value was 7.2 Hz. As a result of the analyzes made in computer environment, 6.7641 Hz was obtained for Mode 1 from tabular data (in ANSYS) as the frequency value.

This shows that the test results in the experimental environment and the analysis results obtained in the computer environment confirm each other.

A displacement amplitude of 0.5 mm was applied to the part in 0.1 Hz increments in the range of 1-10 Hz, and the amplitude of the vibration created by the extreme points of the prototype against the drive was measured. The frequency value with the largest amplitude value was determined as the first free vibration frequency in the 1st bending mode. During the finite element simulations, it was observed that the vibration frequency shifted upwards with the increase in the fixed connection area. From here too; It turns out that any vibration-generating situation that may occur to the lid during take-off and landing of the aircraft can be eliminated by increasing the number of supports. As a result of the test, it was observed how the part would behave in the direction of the applied force and the frequency values were at the expected level.
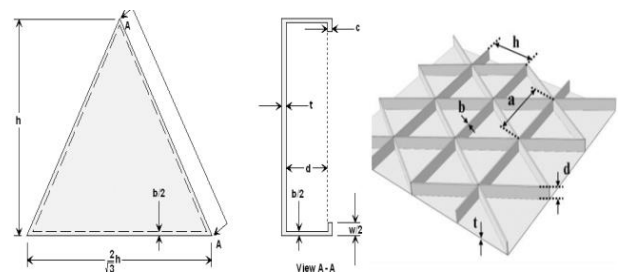
STATIC ANALYSIS RESULTS

Figure -18: Parameters based on the determination of isogrid structure dimensions [2]

a = Rib width   **d =** Rib height

b = Rib thickness   **h** = Cell height

c = Flange thickness   **w** = Flange width

t = Surface plate thickness

In the computer analysis, a distributed load of 964.7 N was applied from the sheet metal part of the designed parts.

The applied force is determined by **Equation 1-2**. For plates such as aircraft landing gear lid, the drag coefficient value is taken as 1.17 [10]. When looking at the existing projects, the equation parameters are taken as listed in **Table 6.**

$$F = C_d \times A \times \sin(\beta) \times q$$

Equation 1-2 [10]

Table -6: Equation parameters as a basis for calculating the load value applied to the aircraft lid [10].

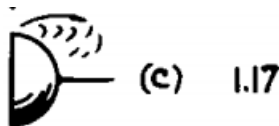| Area [m2]	Cd	Height [ft]	Mach	Dynamic Pressure [Pa]	Angle of Slideslip [Degree]	Force [N]
0,225	1,17	18000	0,55	10714,5	20	964,7

Figure -19: Coefficient of drag effect mechanism [10]

In the analyzes made, the perforated parts were accepted as built-in hinges, as in aircraft lids. A fixation of 100 mm was made from the frame in the area of the isogrid structure. A force of 964.7 N was applied from the sheet metal as a distributed load.

Table -7: Material properties [11]

MATERIAL AA7050-T7451						
Yield Strenght	Tensile Strenght	Elastic Modulus	Poisson Ratio	Mass Density	Modulus of Rupture	Coefficient of Thermal Expansion
4.7e+08 N/m^2	5.25e+08 N/m^2	7.2e+10 N/m^2	0.33	2830 kg/m^3	2.69e+10 N/m^2	2.4e-05 /Kelvin

After that, optimization work was carried out up to 1 mm deformation. An isogrid plane lid design of 1500x150x75 mm with a rib thickness of 1.6 mm has been achieved.

Static analysis results of the designed isogrid lid design are shown in **Figure 4.1** and **Figure 4.3** In order to compare the obtained mass savings, the flat plate design was made by making topology optimization on the flat plate to meet the stress and displacement values in the designed structure. AA7050 T7451 is used as the material. 1500x150x42.5 mm flat plate static analysis results are shown in **Figure 4.2** and **Figure 4.4.**
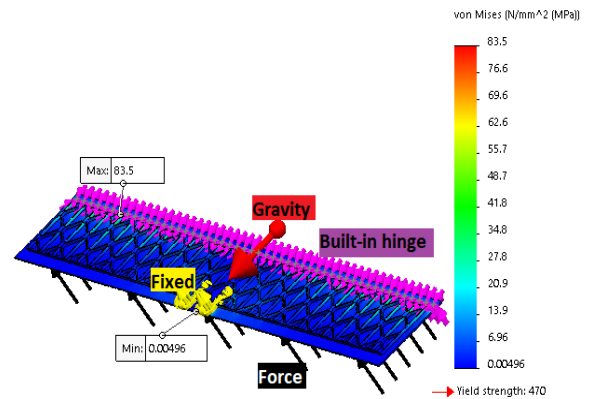
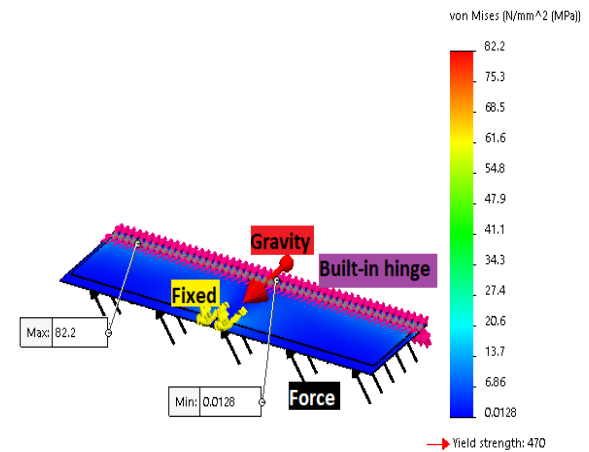**Figure -4.1:** Static Analysis Results for Isogrid Structure Von Mises Stress Data

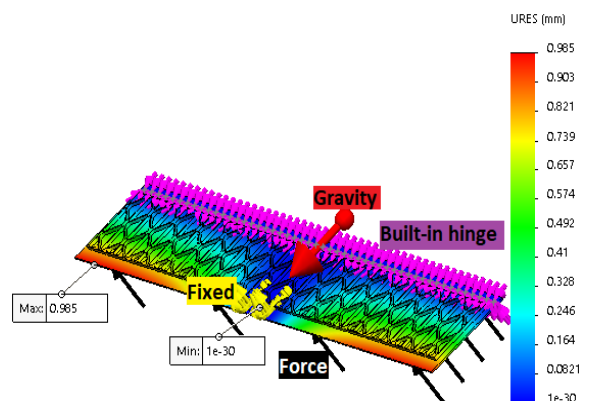**Figure -4.2:** Static Analysis Result Von Mises Stress Data for Flat Plate

Figure -4.3: Displacement Data of Static Analysis for Isogrid Structure
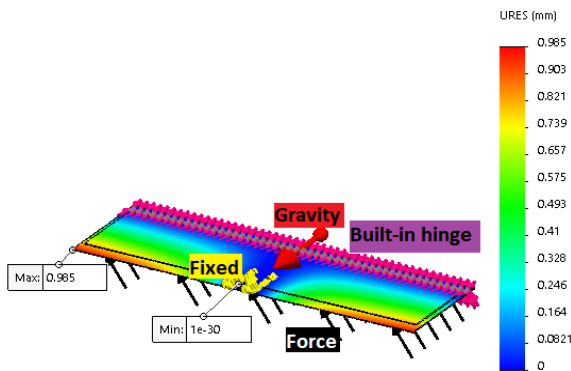
Figure -4.4: Static Analysis Result Displacement Data for Flat Plate

Table -8: Comparison chart for designs with flat plate and isogrid structure

Flat Plate and Isogrid Part Comparison			
	Displacement (mm)	Max Stress (MPa)	Mass (Gram)
Flat Plate	0,985	82,2	2265.36
Isogrid Part	0,985	83,5	1983.99

Flat plate and isogrid structure analysis results at the same boundary conditions are given in **Table 8.**

As a result, the results obtained in the isogrid structure and the static analysis results obtained in the flat plate matched each other. As a result of this study, a mass reduction of 281.37 grams was achieved for the designed landing gear lid. It was observed that 12.42% of mass was saved without loss of strength.

CONCLUSION

In this study, the most suitable isogrid structure design was determined on the landing gear lid, which is an aircraft structural part made of AA7050 T7451 material. The results were verified with the results obtained from computer analysis after performing static analysis, buckling, three-point and free vibration tests. As a result of the vibration tests, it has been revealed that any vibration-generating situation that may occur to the lid during the take-off and landing of the aircraft can be prevented by increasing the number of supports. Compared to the part without the grid structure, a gain of 12.42% was achieved in terms of mass without any loss of strength. The final design of the isogrid structured part, which brings the mass to a minimum without reducing the strength below the critical value, was created. This shows that the aviation and automotive sectors

are in the desired direction to reduce fuel savings and mass-strength optimization. As a result of the optimization work, a lighter lid has been produced and less load will be placed on the mechanism that will open and close the lid. In order to optimize the isogrid building dimensions during the design process, different sized isogrid building designs were made and compared with the analyzes made under the same boundary conditions. In order to minimize the mass, the non-isogrid (plate) part was requested to be as thin as possible. While thinning the plate, static analyzes were repeated frequently, paying attention not to fall below the critical strength point, and as a result of the analyses, it was decided that the plate thickness should be 2.5 mm. The rib measurements of the isogrid structure supporting the plate were also compared with the analyzes and determined by the optimization study. For the final design created, samples were produced and subjected to tests in the laboratory, the results obtained were compared with the analysis results and the analyzes were confirmed. As a result of these studies, it was observed that the most suitable results were obtained when the rib height was 5 mm and the rib thickness was 1.6 mm.

DISCUSSION

As a result of the studies carried out by NITISH GHADI (IRJET August 2017) on composite isogrid structures, the 1000 N force applied as a result of the static analyzes carried out with one side fixed, the stress values of 98.23 MPa and the displacement 9.465 mm were obtained.   As a result of the static analyzes made in this study, it showed lower stress and displacement results than the composite material, since the material used was aluminum.

Considering the stress and displacement results under high G loads affecting aircraft in the aviation industry, AA7050 material offers higher strength and lower displacement compared to composite.

REFERENCES

[1] Design and FE Analysıs of composite grid structure for skin stiffening applications, Nıtısh Ghadı, Prof.Anand Mattikalli, Prof Anant Ghadi, International Research Journal of Engineering and Technology (IRJET)pp. 2127-2130, doi:10.1126/science.1065467.

[2] Meyer RR, Harwood OP, Harmon MB, Orlando JI (1973) Isogrid design handbook. NASA

[3] Hiroaki Kurishita et al., "Fracture Toughness of JLF-1 by Miniaturized 3-Point Bend Specimens with 3.3-7.0 mm thickness".

[4] ASTM Standard, Designation: ASTM ASTM E290 - 14 Standard Test Methods for Bend Testing of Material for Ductility

[5] ASTM Standard, Designation: ASTM E855 – 21 Standard Test Methods for Bend Testing of Metallic Flat Materials for Spring Applications Involving Static Loading

[6] ASTM Standard, Designation: D 790-17 "Standard Test Methods for Flexural Properties of Unreinforced and Reinforced Plastics and Electrical Insulating Materials"

[7] Naceur H, Guo YQ, Ben-Elechi S. Response surface methodology for design of sheet forming parameters to control springback effects. Computers &. Structures 2006;84(26-27):1651-1663.

[8] L.W. Rehfield, R.B. Deo, Buckling of Continuous Filament Advanced Composite Isogrid Wide Columns in Axial Compression (Georgia Institute of Technology, 1978)

[9] Aerospace Science and Technology Volume 24, Issue 1, January–February 2013, Pages 198-203 Analysis of the effect of stiffener profile on buckling strength in composite isogrid stiffened shell under axial loading G.H.Rahimi , M.Zandi , S.F.Rasouli

[10] Hoerner, sighard F,1906-Fluid-dynamic drag. MidlandPark, NJ. Dr. ıng.S.F. Hoerner, 1958 (Page 3-17)

[11] Metals Handbook, Vol.2- Properties and Selection: Nonferrous Alloys and Special-Purpose Materials, ASM International 10th Ed. 1990.

BIOGRAPHIES

Name Surname: Mahmut ALKAN
Address: Fethiye District, Aviation Boulevard No:17 06980 Kahramankazan Ankara / TURKEY

Name Surname: Umut CAN
Address: Asagi Kayabası Street Avenue Gökkuşagı D block Floor: 3 No: 9 Nigde/Center/TURKEY

Name Surname: Sinan Barkin KOCADAG
Address: Kendirli Asiyan Apartment Floor: 2 No: 8 Nigde/Bor/TURKEY

Name Surname: Ahmet Alp SUNECLI
Address: Saltuk Street. 281. D5-B Apt. No: 2 Nigde/Bor/TURKEY

Name Surname: Erhan CELIK
Address: Asagi Hisar Street 4599. No: 15/3 Antalya/ Manavgat/TURKEY